Available online at www.sciencedirect.com
ScienceDirect
Chemical Physics 341 (2007) 336–343
Chemical Physics
www.elsevier.com/locate/chemphys

Chirped molecular vibration in a stilbene derivative in solution

Anne Colonna [a,b], Atsushi Yabushita [a,c,*], Izumi Iwakura [d,e], Takayoshi Kobayashi [a,c,e,f,g]

[a] Department of Physics, Faculty of Science, University of Tokyo, Hongo 7-3-1, Bunkyo-ku, Tokyo 113-0033, Japan
[b] Laboratory for Optics and Biosciences, Ecole Polytechnique, 91128 Palaiseau Cedex, France
[c] Department of Electrophysics, National Chiao Tung University, Hsinchu 300, Taiwan
[d] JSPS Research Fellow, 8 Ichibancho, Chiyoda-ku, Tokyo 102-8472, Japan
[e] Department of Applied Physics and Chemistry and Institute for Laser Science, University of Electro-Communications, 1-5-1 Chofugaoka, Chofu, Tokyo 182-8585, Japan
[f] JST, ICORP, 4-1-8, Kawaguchi-shi, Saitama 332-0012, Japan
[g] Institute of Laser Engineering, Osaka University, 2-6 Yamada-oka, Suita, Osaka 565-0971, Japan

Received 1 March 2007; accepted 29 August 2007
Available online 12 September 2007

Abstract

The wave packet dynamics of 4-methoxy-4′-nitrostilbene in solution was studied by femtosecond pump–probe spectroscopy. Transient changes in absorbance exhibit oscillations, which reflect vibrational motions on the ground-state potential surface. Modification of this oscillatory feature in three different solvents (benzene, methanol, and acetonitrile) can be explained in term of the strength of hydrogen bonding and the stabilization of charge-transfer state, confirmed by steady-state absorption and fluorescence spectra.

Keywords: Ultrafast spectroscopy; Stilbene; Photoisomerization

1. Introduction

Advance in femtochemistry opens a way to study ultrafast dynamics in chemical reactions with high time resolution. Photoisomerization is one of the most important reactions and is highly related to important photobiological processes such as vision. However, the description of the process is complicated because of high degree of freedom due to many vibration modes [1–3]. Stilbene and its derivative have been extensively studied as a standard reference system for *cis*-trans photoisomerization ([4–7]). In *cis*-stilbene, the photoisomerization process finishes rapidly in 1 ps [8,9]. The photoisomerization also occurs in *trans*-stilbene but it takes almost 100 ps because there is a potential barrier on the way to transform into an intermediate state twisted at about 90° around its ethylene bond [10]. Various experimental and theoretical studies have been carried out to propose models explaining the relaxation process [11,12]. Stilbene derivatives appear to be useful to probe the electronic nature and to discriminate between singlet versus triplet mechanism, since the ratio of their contributions are highly dependent on the substituents [13].

Even though the photoisomerization of stilbene involves 72 modes, the relaxation process in the molecule has been understood to be described in a simplified way in a two-dimensional view, involving θ (double bond torsional angle) and ϕ (phenyl ring rotation angle) torsional angle [14–17]. Reaction toward twisting can be monitored by ultrafast spectroscopy, and nuclear motions on the potential energy surface are followed with high temporal resolution [18].

In the present letter, we report the wave packet motion in 4-methoxy-4′-nitrostilbene in three solvents (methanol, acetonitrile, and benzene) with different polarities and proticity. This molecule contains both electron donor and

* Corresponding author. Address: Department of Physics, Faculty of Science, University of Tokyo, Hongo 7-3-1, Bunkyo-ku, Tokyo 113-0033, Japan. Fax: +81 3 5841 4240.
E-mail address: yabushita@mail.nctu.edu.tw (A. Yabushita).

0301-0104/$ - see front matter
doi:10.1016/j.chemphys.2007.08.028

acceptor groups, enhancing the presence of a charge-transfer excited state [19,20]. Results are consistent with the formation of this state stabilized by the solvent polarity.

To study nuclear motions, we monitor wave packet motions on the potential energy surface, with ultrafast time resolution. Oscillatory signal observed was dependent on solvent dielectric constant and proticity. Molecular vibration frequency was found to be time dependent, and it is called as chirped molecular vibration in the present letter. The terminology ''chirped'' means a frequency of an oscillating phenomenon is time dependent, and the chirping can be generally found in many oscillating systems, as studied by sonogram [21] in acoustics and spectrogram in ultrashort pulse optics [22]. The solvent dependence of the chirp rate of the molecular vibration was discussed in terms of the strength of hydrogen bonding and the electronic energy stabilization of the charge-transfer state. We present results of a pump–probe experiment where probing occurs at a single frequency. A time-dependent frequency of the wave packets was analyzed by assuming that oscillatory contributions are caused solely by vibrational wave packet motions in the electronic ground state.

2. Experimental

Reagent grade *trans*-4-methoxy-4′-nitrostilbene (MONS) (Tokyo Kasei: guaranteed) was dissolved in spectro-grade solvents with different polarities (benzene, acetonitrile, and methanol) without further purification. The electronic absorption spectra agreed well with those reported. All samples had an optical density of about 1.0 at 395 nm in a 1-mm cell (6210-27501; GL Science) used for femtosecond experiment (concentrations in the range from 10^{-5} to 10^{-4} M). The solutions were carefully prepared monitoring their absorption spectra by an ultraviolet–visible–near-infrared (UV–VIS–NIR) scanning spectrophotometer (UV-3101PC; Shimadzu). It was confirmed that the sample consists 98% of *trans*-MONS by NMR.

A Ti:sapphire laser system (FemtoSource (sPRO); FemtoLasers) with an 8-path bow-tie amplifier (FemtoPower; FemtoLasers) was used for pump–probe experiment [23]. The width, energy, spectral range, and repetition rate of the pulses were 20 fs, 30 μJ, 750–870 nm, and 1-kHz, respectively. The output fundamental pulse was frequency doubled to generate a 395 nm pulse having a width of 40 fs at the 1-kHz repetition rate. The output pulse was split into two parts (pump and probe pulses) and focused by a parabolic mirror into a standard fluorimeter cells (6210-27501; GL Science). Time delay of the probe pulse with respect to the pump pulses was changed by an electrically driven stepper with a 10-fs step.

Fluorescence emission and excitation spectra were measured with a fluorescence spectrophotometer (F-4500; Hitachi). Changes in the quantum yield and shift in the fluorescence-emission spectra were observed in the three solvents. Fluorescence emission spectrum for each sample was obtained for different excitation wavelengths between 500 nm and 700 nm and between 320 nm and 470 nm. All measurements were performed at room temperature (294 K ± 1).

3. Results and discussion

3.1. Steady-state absorption and fluorescence spectra

Experimental results summarized in Table 1 show that absorption peak wavelength, fluorescence quantum yield, and wavelength of emission maximum depend on solvent polarity, because in the emission process a gigantic dipole moment is involved in the lowest excited singlet state.

Fig. 1 shows the fluorescence and absorption spectra of MONS in three different solvents (acetonitrile, benzene, methanol). In fluorescence and absorption peak photon energies, there are differences between the benzene (dielectric constant $\varepsilon = 2.3$) solution sample and acetonitrile ($\varepsilon = 37.5$) solution sample. The difference (1913 cm^{-1}) of fluorescence peaks is about two times larger than that (1040 cm^{-1}) of absorption peaks. It is due to larger dipole moment induced be increased amount of charge-transfer due to extended electron density in the excited state than in the ground state in all of the solvents. The calculated dipole moment for MONs in vacuum in the excited state was 9.1 debye with CIS/6-31G* and in the ground state was 7.5 debye with MP2/6-31G*. Even layer difference

Table 1
Fluorescence maxima (λ_F), Stokes shifts (SS), fluorescence quantum yields (ϕ_F), radiative lifetimes (τ_0), solvent refractive indices (n), radiative (k_r) and non-radiative (k_{nr}) rate constants and fitting parameters (γ^{-1}, r, a/b, and T_o) to $M(t)$ defined by Eq. (4) describing the dumped molecular vibration of MONS in several solvents with different dielectric constants (ε)

Solvent	ε	λ_{abs} (nm)	λ_F (nm)	SS (cm^{-1})	ϕ_F	τ_o (ns)	N
Acetonitrile	37.5	374	596	9959	0.06	6.6	1.342
Methanol	32.6	372	590	9933	0.01	5.8	1.329
Benzene	2.3	360	535	9086	0.004	3.9	1.501
	k_r (10^8 s^{-1})	k_{nr} ($10^9 s^{-1}$)	γ^{-1} (fs)	a/b	$1/cT_o$ (cm^{-1})	r	Viscosity (mPa/s)
Acetonitrile	1.5	2.4	334	3.7	175	0.45	0.35
Methanol	1.7	17.1	620	5.2	238	0.43	0.61
Benzene	2.5	63.8	265	2.0	137	0.48	0.649

All values were obtained at room temperature (294 K ± 1).

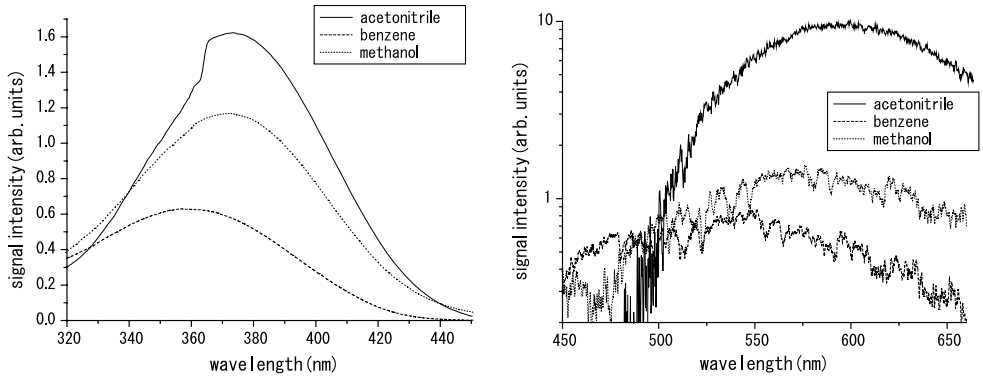

Fig. 1. Absorption (left) and emission (right) spectra of MONS in three different solvents.

can be expected in solution especially in polar solvent. Compared among the cases of all of the solvents, the Stokes shifts were even more enhanced in more polar solvents [24].

Red shift in fluorescence emission maximum on going from benzene to acetonitrile is attributed to an increased reduction in the energy level of the excited state with solvent polarity achievable by intramolecular charge transfer relaxation out of the locally excited (LE) state [25]. Fluorescence quantum yield is the ratio of photons emitted to photons absorbed and can be expressed as follows:

$$\phi_F = k_r/(k_r + k_{nr}). \quad (1)$$

Here k_r and k_{nr} are the rate constants of the radiative and non-radiative relaxation, respectively. In the present case, relaxation modes are considered to be dominated by internal conversion and isomerization from the previous study [4]. The viscosity dependence of the isomerization rate was previously studied using time-resolved absorption [26,27], and the result shows that the isomerization rate decreases as the viscosity increases. It causes the increase of fluorescence quantum yield as a function of solvent viscosity. This is in contraction to the observation, but the change in the viscosity is very small. Hence the other effects such as solvent polarity may change the radiative rate resulting in the change in the efficiency.

The excited-state population is expected to decay into other states by radiative or non-radiative processes with a lifetime

$$\tau = 1/(k_r + k_{nr}). \quad (2)$$

The radiative rate constant was calculated using the Strickler and Berg formula [28]

$$k_r = 1/\tau_0 = 2.880 \times 10^{-9} n^2 \langle \nu_f^{-3} \rangle_{AV}^{-1} \frac{g_l}{g_u} \int \varepsilon d\ln \nu_a. \quad (3)$$

Here g_l and g_u are the degeneracies of the lower and upper electronic state, respectively (both equal to unity in this case), n is the refractive index of the medium (we are using the refractive index of the solvent since MONS concentration is very small), ε is the molar extinction coefficient. ν_f and ν_a are the frequencies of the fluorescence emission spectrum and absorption spectrum, respectively, expressed in wavenumber. Integration is performed over the electronic absorption band.

3.2. Femtosecond dynamics

Fig. 2 shows the time dependent absorbance change (ΔA) induced by excitation of MONS with femtosecond pulses. There was almost no change in the absorption spectrum of the sample solution before and after femtosecond experiments. All of the sample have positive sign signal just after the zero-delay position, however the lifetime of the signal is shortest in the case of benzene. Therefore the positive sign signal cannot be observed in the left figure of the benzene data in Fig. 1 because of the low time resolution.

In the same way as for *cis*-stilbene, our pump probe data on MONS shows both exponential decay and oscillatory pattern (Fig. 2). From Fig. 2 it is easily seen that the electronic dynamics can be expressed by a two-component exponential function. For the analysis of molecular vibration, shorter delay time range than 1 ps was used. In this range the longer decay time (>10 ps) behavior does not affect the analysis. The fine structures in the curves are partly due to noise in the data and partly due to molecular vibration that is dominant in the delay time ranges from just after excitation to about 500 fs. To clearly observe the fine structures, sub-ps time dependence related to electronic dynamics was subtracted from the real-time trace observed for MONS in benzene (Fig. 2 topmost figure). The obtained fine structures are shown as thin curves in Fig. 3 exhibiting non-sinusoidal dependence on probe delay time. The observed fine structures are discussed in the following.

The observed fine structure shows that the vibrational frequency of the signal becomes lower in larger delay time. When multiple modes are active, the data can be explained without resorting to chirp. However, as was studied in [29], there is only one intensive mode around the vibrational frequency observed in the present work. Therefore we analyzed the data by taking the change of the vibrational frequency as a chirp of the frequency. The observed chirp rates were dependent on the solvent. The possible reason

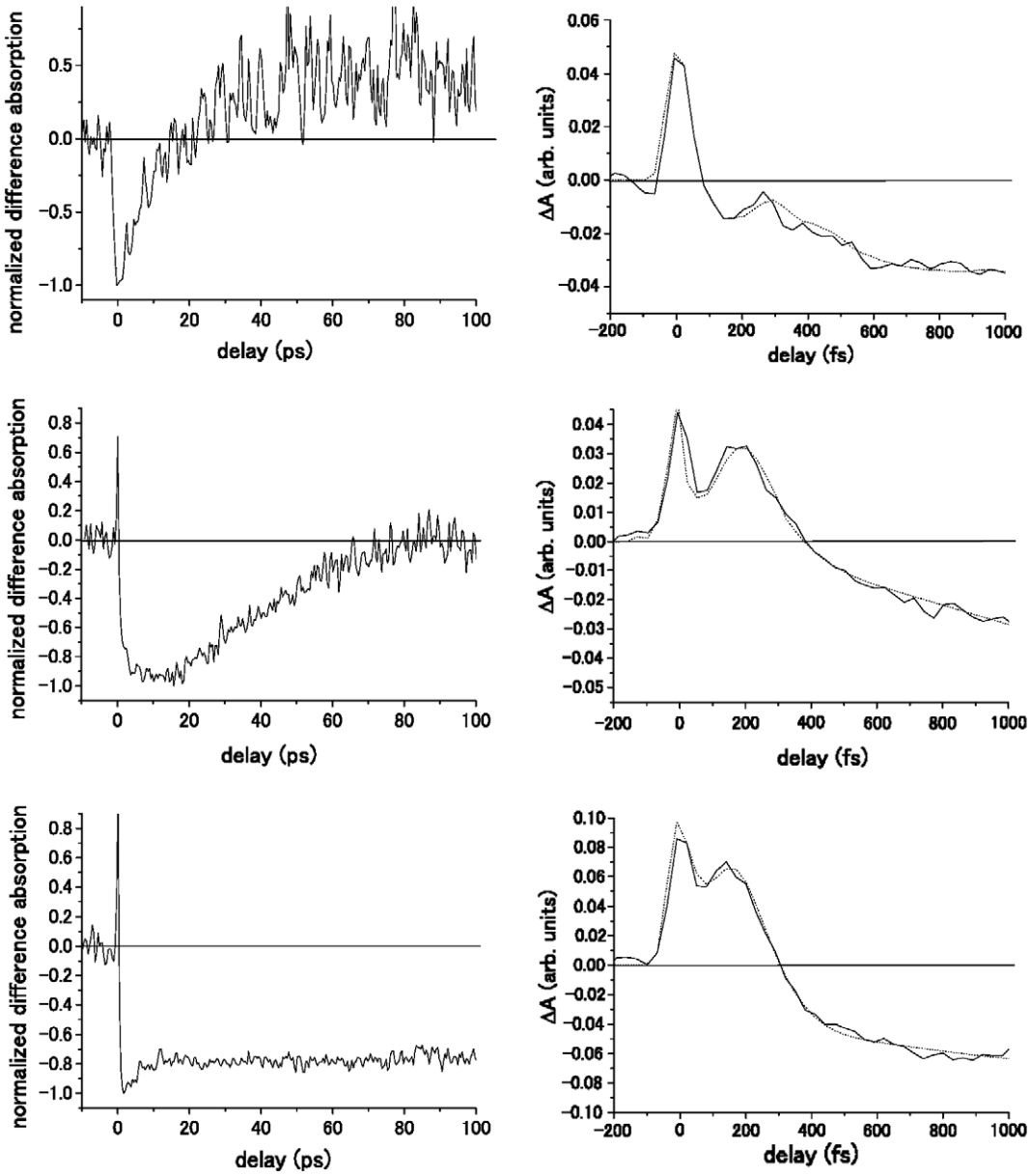

Fig. 2. Femtosecond transient absorbance change (ΔA) against probe delay time up to 100 ps (left column) and 1 ps (right column) of MONS in three different solvents. Smooth line is the best fitting. From top to bottom: benzene, methanol, and acetonitrile.

of the phenomena is given in the end of the following discussions.

Many years ago, a simplified model of potential energy surface (PES) was used to analyze *cis*-stilbene [9]. Now it is available to calculate PES numerically even for *trans*-MONS, which has more, complicated lateral chain compared with the *cis*/*trans*-stilbene. Therefore we performed a quantum mechanical calculation to obtain the PES, the result of which is shown in Fig. 4. In the calculation of the PES, we have assumed phenyl ring rotation angle $< C^1–C^2–C^3–C^4$ (ϕ_1) = $< C^2–C^1–C^5–C^6$ (ϕ_2) for the simplicity of the calculation.

In the present work, the simulated curves calculated from the PES were represented well with the following response function of signal intensity against the probe delay time with a chirped vibrational frequency

$$M(t) = \exp(-\gamma t) \cdot \left[a + b \cdot \cos\left(\frac{2\pi}{T_o + rt} \cdot t \right) \right]. \quad (4)$$

Here, γ is the decay time of the molecular vibration in the ground state and a and b are proportionality constants of the pure electronic contribution and the vibrational contribution. T_o is the oscillation period of the molecular vibration. This response function was also used to fit measured data for *cis*-stilbene [9]. In Fig. 3 the simulated curves obtained from the calculated PES (thick curves) fit well with the measured fine structures (thin curves). We used Eq. (4) to fit the observed fine structures in the time region

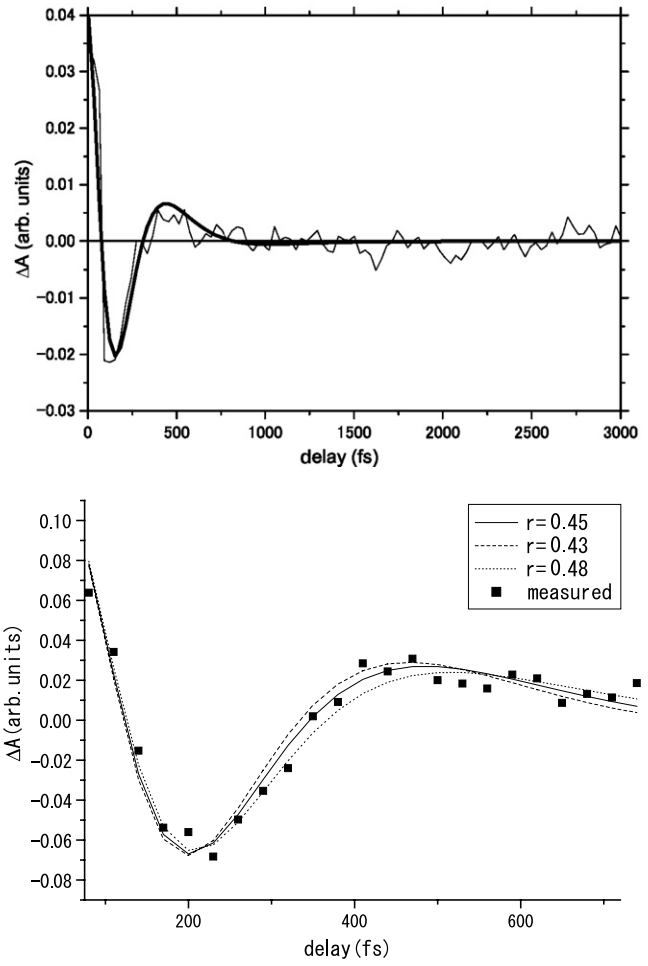

Fig. 3. (Top) Thin curve: Probe delay time dependence of ΔA (real-time trace) observed for MONS in benzene (Fig. 2 topmost figure) after removal of slowly varying time dependence. Thick curve: Numerically simulated curve obtained from the calculated potential energy surface (PES). (Bottom) Filled squares: Probe delay time dependence of ΔA observed for MONS in acetonitrile (Fig. 2 middle row figure) after removal of slowly varying time dependence. Thin lines: Fitted curves using the parameters shown in Table 1 scanning the value of r.

from −200 to 1000 fs as shown in Fig. 3. Immediately after photoexcitation, the vibration cycle with respect to θ at $\phi = -26$, which is most stable in the ground state, is 244 fs from the experiment result. The chirp rate $r = 0.56$ of the θ vibration was determined by the calculated PES. This rate is close to the observed ones listed in Table 1.

Of course, it is desirable to obtain analytical expression for the time dependence of the dynamic absorbance change. However, it is extremely difficult not only to derive an analytical expression but also to obtain numerical result including numerous solvent molecules with high polarizabilities and thermal molecular vibrations. Therefore we took the same phenomenological expression as was successfully applied to the gas phase stilbene. Even though Eq. (4) is a phenomenological equation, it can be supported by the following discussion.

The coupling between the relevant mode and many other modes introduced by the impulsive excitation can be given by the bilinear coupling in the lowest order approximation. Then the oscillation frequency can be modified linearly with the most strongly coupled mode in case the latter is much slower than the relevant mode frequency.

Eq. (4) represents the chirped molecular vibration whose oscillation period changes linearly with delay time with rate of r. The vibrational dephasing and population decays are assumed to be much longer than $1/r$ and $1/T_o$. It shows phenomenological energy dissipation, which takes place both *via* intramolecular and intermolecular interactions. The former is due to mode coupling among the molecular vibration modes in each molecule. The latter is due to intermolecular interaction especially van der Waals interaction between the vibronic transition with the same transition energies between the neighboring molecules. For the sake of simplicity, we assumed that the energy loss rate through the channel is constant in such short probing time as <4 ps and the averaged instantaneous frequencies of low-frequency modes decreases linearly with elapsing time. For the analysis this function was convoluted with the laser response function. Referring the measurement results shown in [4] of *trans*-stilbene, we found two candidates of the origins of the observed molecular vibration. One of the origins is the deformation of $C^1{=}C^2{-}C^3$ in the center of this molecule. It was observed as a vibration whose oscillation frequency is 200 cm^{-1} in the measurement of *trans*-stilbene [4,29]. However, the oscillation frequency is not chirped unlike the case observed in the present work. Therefore the observed chirped molecular vibration was attributed to another origin of the chirped molecular vibration, namely torsional mode θ [30] as is shown in the following paragraphs. This is supported to the theoretical result as follow. The optimized structures of θ in the ground state and excited state were different. And so, it is thought that θ is Franck–Condon revitalization. Table 1 summarizes these parameters for MONS in three different solvents.

The mechanism of the negative chirp of molecular vibration is discussed in terms of the wave packet motion in the ground state. After photoexcitation, both wave packets in the excited state and the ground state can be formed. In the present case the pump laser spectrum covers only the edge of the absorption spectrum of MONS and the generation of the excited state wave packet is expected to be much less effective than that of the ground state [31].

To clarify the dynamics of wave packet generated in MONS by the femtosecond pulses we performed a quantum mechanical calculation. The most stable structures of MONS were calculated in the ground and the lowest excited states (Fig. 5). The calculation[1] was performed using MP2/6-31G* and CIS/6-31G* level. It shows that MONS has a twisted angle ϕ of −25.9° in the ground state. However, in the lowest excited state, the angle of ϕ becomes 0° and the geometrical structure is almost planer

[1] Gaussian 03, Revision D.02; Gaussian, Inc., Wallingford CT, 2004.

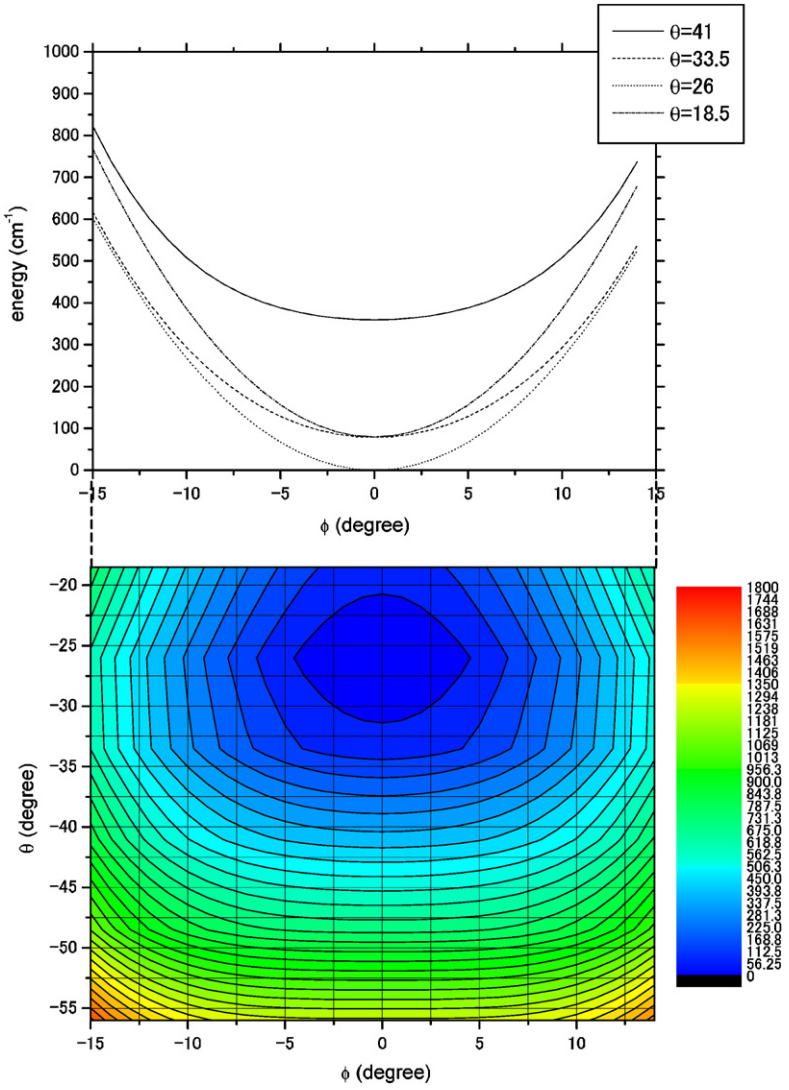

Fig. 4. (Bottom) Contour map of the potential energy surface (PES) of MONS in the ground state calculated using MP2/6-31G* and CIS/6-31G* level (Gaussian 03, Revision D.02; Gaussian, Inc., Wallingford CT, 2004.). The four horizontal thick lines are corresponding to the phenyl ring rotation angles $\phi(\phi_1 = \phi_2)$ shown on the top of the figure. (Top) shows cross-sections of the potential energy surface.

linear. The structure of the potential energy surface (PES) of MONS was also calculated for the ground state (Fig. 4). This result is going to be used to compare with the experimental results measured with MONS solved in benzene. The dielectric constant of benzene is so small that effect of solvent is not effective. Therefore the calculation of Fig. 4 was done in vacuum condition neglecting the effect of solvent. When the population of MONS molecules in the ground state is shifted to the Franck–Condon region in the excited state, it starts to increase the angle of ϕ bound for the most stable structure of the excited state. As a counter action of the motion of excited state wave packet, the wave packet in the ground state MONS starts to move decreasing ϕ. From the fact that the phase of the vibration the real-time signal is considered mainly due to the wave-packet motion in the ground state. Fig. 4 shows when ϕ decreases in the ground state the curvature of the PES also decreases, which causes the chirp in the molecular vibration frequency as seen in Fig. 3.

As seen in the bottom figure of Fig. 3, the chirping parameter of MONS solved in acetonitrile is 0.45, which is intermediated value between that of MONS solved in benzene ($r = 0.48$) and that of MONS solved in methanol ($r = 0.43$). Because of the low signal to noise ratio, the obtained chirping parameters also include noise, but, at least, we could show that the chirping parameters are dependent on solvents as above. Here the difference in the chirping parameters is to be discussed. Since the time scales and impact of the rearrangement of the solvent shells (solvation dynamics) is strongly dependent on the solvent used, it has major influences on the pump–probe response, as is also observed in chirped wave packet dynamics of HgBr in [32]. In the cases of benzene and acetonitrile, differences can be accounted for large difference in their dielectric constant. Since acetonitrile and methanol have similar dielectric constants, the following is thought to be a possible explanation of the difference in the parameter. The presence of –OH group in methanol is expected to

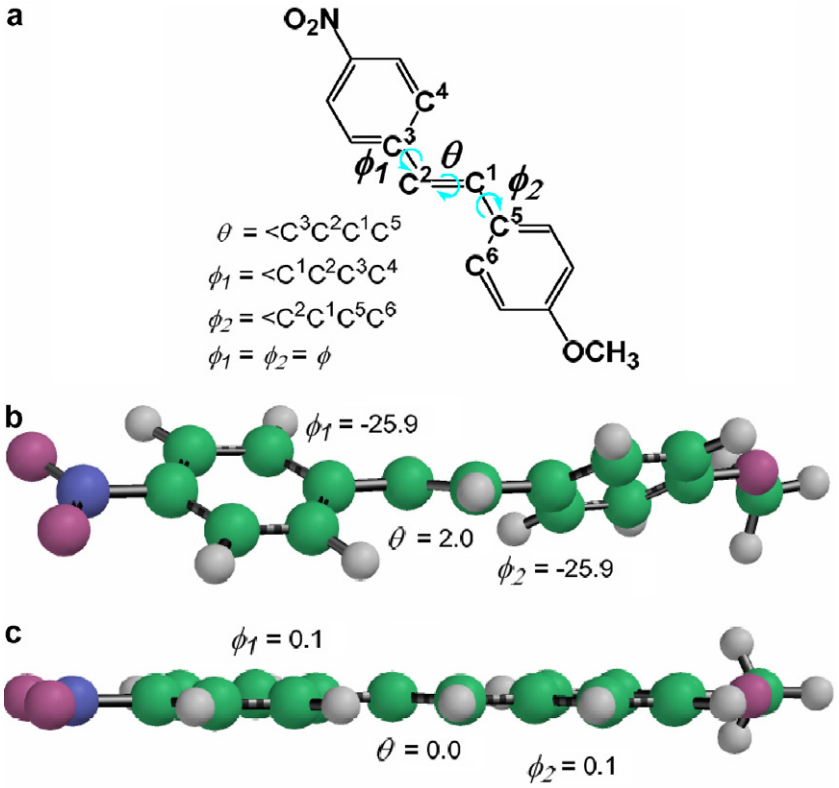

Fig. 5. (a) Constitutional formula of MONS. The most stable structures of the MONS were calculated for (b) ground and (c) excited states.

form hydrogen bonding via the π-electron system by a partial charge-transfer (CT) mechanism. Therefore, the shorter T_o in methanol is explained in terms of the increase in the force constant of the C=C bond stretching being fixed by the locking of the structure by the hydrogen bonding.

In conclusion, we could observe the chirped molecular vibration on the ground-state potential surfaces in a condensed phase for the first time. The dependency of the chirp rates on solvents is well explained in terms of the differences in the dielectric constant and/or proticity of the solvent. We are now in the process of extending this work to many solvents with different parameters of polarity and refractive index, targeting systematical study by introducing theoretical investigation [1,20,33].

Acknowledgements

The authors would like to acknowledge Prof. Eiji Tokunaga for his valuable discussion. This work was supported by ICORP program of Japan Science and Technology Agency (JST), a fellowship of JSPS Summer Program, a Grant-in-Aid for Specially Promoted Research (14002003) from the same ministry and specific allowances from the Japan Society for the Promotion of Science, the grant MOE ATU Program in NCTU, and a Grant-in-Aid for Science Research in a Priority Area "Super-Hierarchical Structures" from the Ministry of Education, Culture, Sports, Science and Technology, Japan. We also thank the Information Technology Center of University of Electro-Communications for their support of the theoretical calculation.

References

[1] D.E. Lippert, W.L. Lüder, F. Moll, W. Nägele, H. Boos, H. Prigge, I. Seibold-Blankenstein, Angew. Chem. 73 (1961) 695.
[2] J.B. Birks, Chem. Phys. Lett. 38 (1976) 437.
[3] V. Molina, M. Merchàn, B.O. Roos, J. Phys. Chem. A 101 (1997) 1552.
[4] D.H. Waldeck, Chem. Rev. 91 (1991) 415.
[5] T. Kobayashi, E.O. Degenkolbl, P.M. Rentzepis, J. Appl. Phys. 50 (1979) 3118.
[6] S.K. Kim, S.H. Courtney, G.R. Fleming, Chem. Phys. Lett. 159 (1989) 543.
[7] H. Görner, D. Schulte-Frohlinde, Ber. Bunsenges. Phys. Chem. 82 (1978) 1102.
[8] B.I. Greene, R.C. Farrow, J. Chem. Phys. 78 (1983) 3336.
[9] S. Pedersen, L. Banãres, A.H. Zewail, J. Chem. Phys. 97 (1992) 8801.
[10] G. Rothenberger, D.K. Negus, R.M. Hochstrasser, J. Chem. Phys. 79 (1983) 5360.
[11] E. Wei-Guang Diau, J. Phys. Chem. 108 (2004) 950.
[12] R. Lapouyade, A. Kuhn, J.F. Letard, W. Rettig, Chem. Phys. Lett. 208 (1993) 48.
[13] D.V. Bent, D. Schulte-Frohlinde, J. Phys. Chem. 78 (1974) 446.
[14] J.C. Polanyi, A.H. Zewail, Acc. Chem. Res. 28 (1995) 119.
[15] M. Terauchi, T. Kobayashi, Chem. Phys. Lett. 137 (1987) 319.
[16] A.Z. Szarka, N. Pugliano, D.K. Palit, R.M. Hochstrasser, Chem. Phys. Lett. 240 (1995) 25.
[17] A.B. Myers, R.A. Mathies, J. Chem. Phys. 81 (1984) 1552.
[18] A.H. Zewail, M. Dantus, R.M. Bowman, A. Mokhtari, J. Photochem. Photobiol. 62 (1992) 301.

[19] J. Oberl'e, E. Abraham, G. Jonusauskas, C. Rulli'ere, J. Raman Spectrosc. 31 (2000) 311.
[20] U. Jentschura, E. Lippert, Akademische Verlagsgesellschaft, Frankfurt am Main (1971).
[21] L. Cohen, Time-Frequency Analysis, Prentice-Hall PTR, Englewood Cliffs, New Jersey, 1994.
[22] J.C. Diels, Ultrashort Laser Pulse Phenomena, Academic Press (1996).
[23] T. Taneichi, T. Fuji, Y. Yuasa, T. Kobayashi, Chem. Phys. Lett. 394 (2004) 377.
[24] M.N. Pisanias, D. Schulte-Frohlinde, Ber. Bunsenges. Phys. Chem. 79 (1975) 662.
[25] S.A. Kovalenko, N.P. Ernsting, J. Ruthmann, Chem. Phys. Lett. 258 (1996) 445.
[26] S. Abrash, S. Repinec, R.M. Hochstrasser, J. Chem. Phys. 93 (1990) 1041.
[27] L. Nikowa, D. Schwarzer, J. Troe, J. Schroeder, J. Chem. Phys. 97 (1992) 4827.
[28] S.J. Strickler, R.A. Berg, J. Chem. Phys. 37 (1962) 814.
[29] S. Takeuchi, T. Tahara, Chem. Phys. Lett. 326 (2000) 430.
[30] T. Kobayashi, S. Saito, H. Ohtani, Nature 414 (2001) 531.
[31] C.J. Bardeen, Q. Wang, C.V. Shank, Phys. Rev. Lett. 75 (1995) 3410.
[32] M. Lim, M.F. Wolford, P. Hamm, R.M. Hochstrasser, Chem. Phys. Lett. 290 (1998) 355.
[33] C. Reichardt, Angew. Chem. Int. ed. Engl. 18 (1979) 98.